Electronic structures of GaP(100) surface reconstructions probed with two-photon photoemission spectroscopy

Philipp Sippel,* Oliver Supplie, Matthias M. May, and Rainer Eichberger
Helmholtz-Zentrum Berlin für Materialien und Energie, Institute for Solar Fuels, Hahn-Meitner-Platz 1, D-14109 Berlin, Germany

Thomas Hannappel
Technische Universität Ilmenau, Institut für Physik, Postfach 100565, D-98684 Ilmenau, Germany
(Received 18 October 2013; revised manuscript received 21 February 2014; published 28 April 2014)

The electronic structures of two significant atomically well-defined (100)-surface reconstructions of gallium phosphide were investigated with two-photon-photoemission spectroscopy (2PPE). We allocated a series of occupied and unoccupied surface states and deduced the influence of each particular reconstruction on the electronic structure of the surface. Photoemission signals arising from bulk optical transitions were distinguished from surface-state related signals by studying the influence of oxygen exposure to the surfaces and by comparing our results to reflectance anisotropy spectroscopy (RAS) measurements. This revealed that the features in the RAS signal correlate with the transition energies between unoccupied and occupied surface-related states that were observed in the 2PPE measurements. An anisotropy around the E_0' critical point, previously known from RA spectra, was also investigated with 2PPE and is ascribed to modifications of the bulk electronic structure in the vicinity of the surface.

DOI: 10.1103/PhysRevB.89.165312 PACS number(s): 73.20.At, 78.55.Cr, 79.60.Bm

I. INTRODUCTION

Hydrogen generation by photoelectrolysis is currently a topic of heavy research [1,2]. In the search for appropriate absorber materials, GaP increasingly receives attention [3], notably because of its wide band gap in comparison to other III-V semiconductors. Further advantages of GaP lie in the possibility of pseudomorphic heteroepitaxial growth on silicon [4,5], which can be even conducted lattice matched, if the material is diluted with nitrogen [6–8]. Since Si(100) has already been established as a foundation of the semiconductor industry and as the photoelectric reaction is a surface phenomenon, the (100) surface of GaP is particularly interesting and a detailed understanding of its properties promises great benefits to the design of the desired (opto)electronic devices. While the morphologies of GaP(100) surfaces have been studied in great detail [9–11], the electronic structures have mostly been an issue for theoretical treatment [12–14] and little experimental data are available [15,16]. The effect of oxygen and water adsorption on the electronic structure of GaP(100) surfaces was recently calculated [17,18] and for water absorption also investigated experimentally [19].

Here, we used two-photon photoemission spectroscopy (2PPE) with femtosecond laser pulses to investigate the electronic structure of the well-defined and well-established [11,20] Ga-rich (2×4) and P-rich $(2 \times 2)/c(4 \times 2)$ surface reconstructions of GaP(100). The surfaces (called Ga rich and P rich, respectively, in the following) were prepared with metal organic vapor phase epitaxy (MOVPE). Reflection anisotropy spectroscopy (RAS) was employed *in situ* during the preparation to verify high sample quality and *ex situ* as an indirect probe for the electronic structure of the surfaces. Structural properties and preparation details of these surface reconstructions of GaP(100) have already been the subject of several studies in the last years [21]. While the Ga-rich surface has been found to be terminated by mixed dimers of gallium and phosphorus atoms on top of a pure Ga layer, the P-rich surface is terminated with hydrogen stabilized phosphorus dimers [13]. Schematics of the atomic structures of both surface reconstructions are shown as insets in Fig. 1.

2PPE allows the simultaneous study of occupied and unoccupied states and has been applied increasingly in the last two decades to investigate the electronic structure of semiconductor surfaces. Much focus has been put on silicon surfaces [22–24] in the past, while studies on III-V surfaces are quite scarce [25–27]. Main challenges are the preparation of atomically well-defined surfaces and the transfer of the samples without any contamination to the actual 2PPE setup, where the sample is in ultrahigh vacuum (UHV). Here, a custom-built MOVPE-to-UHV-transfer system [28] allows the study of samples in the condition provided directly after the preparation.

By comparing two different surface reconstructions of GaP(100), we can distinguish surface- from bulk-related features and discriminate differences between the surface electronic structures. Besides measuring clean surfaces immediately after the preparation, we also measured the same samples after controlled exposure to oxygen. This enables the identification of dangling-bond states and the study of the effect of adsorbed oxygen on the surface electronic structure, allowing a comparison to recent theoretical calculations [17]. We employed RAS, an optical method that is highly sensitive to surface-state transitions [29,30], under identical experimental conditions and discuss similarities between the results of both methods.

II. EXPERIMENT

The samples were prepared in a modified [28] commercial MOVPE reactor (Aixtron AIX 200). GaP layers of about 600 nm thickness were grown on pieces of either sulfur ($n \approx 4 \times 10^{17}$ cm^{-3}) or zinc ($p \approx 5 \times 10^{17}$ cm^{-3}) doped GaP(100)

*philipp.sippel@helmholtz-berlin.de

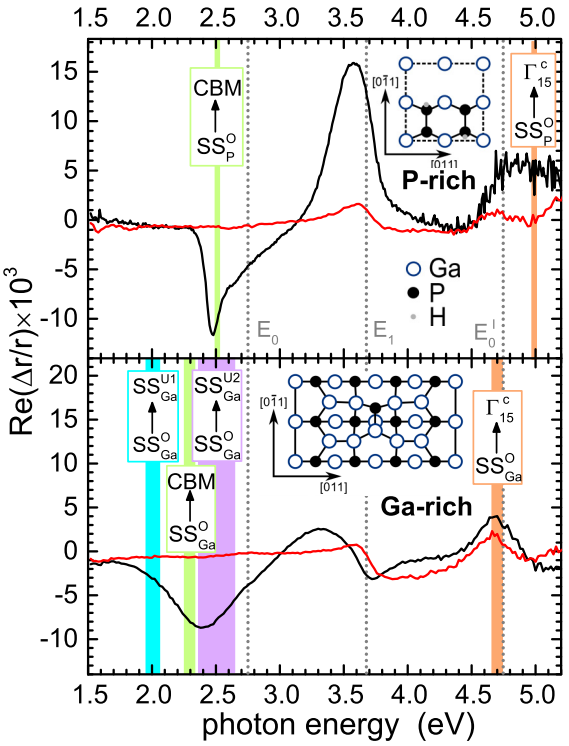

FIG. 1. (Color online) RA spectra of the Ga-rich and the P-rich surface reconstruction, clean (black) and after O_2 exposure (red/grey). The insets show the atomic models of the Ga- and the P-rich surface reconstructions according to Frisch *et al.* [9] and Hahn *et al.* [13], respectively. Dashed lines indicate critical point transitions and vertical bars indicate energy differences between occupied and unoccupied surface states, as well as between occupied surface states and selected bulk states, as identified with 2PPE.

wafers. For the growth process, tertiarybutylphosphine (TBP) and triethylgallium (TEGa) were used as precursors and H_2 as carrier gas. A LayTec EpiRAS RA spectrometer was employed for monitoring and controlling the growth process *in situ*. For deoxidation, the sample was annealed at 650 °C with constant TBP flow to stabilize the surface, while the actual homoepitaxial film growth was conducted at 620 °C. To achieve a P-rich surface reconstruction, the sample was cooled down with TBP stabilization and annealed at 420 °C without TBP. For the preparation of Ga-rich surfaces, samples were subsequently annealed for 5 min at 700 °C without any precursor supply. Given temperatures were measured with a thermocouple placed inside the susceptor. During all steps, RAS was used to control the surface preparation *in situ*. Detailed descriptions of the preparation steps, as well as the MOVPE and RAS setups, have been reported elsewhere [11,21,28,31]. To avoid contamination of the surfaces, the samples were transferred from the reactor environment directly to UHV and afterwards transported to another UHV chamber with a base pressure of approximately 5×10^{-10} mbar, where the actual 2PPE experiments were conducted. This was done without the sample leaving the UHV by using a custom-designed transfer system, including a mobile UHV chamber [28] with a base pressure of approximately 4×10^{-10} mbar.

As light source for these measurements, a commercial (*Coherent*) regenerative amplified Ti:sapphire laser system with a repetition rate of 150 kHz was used, providing pulses of 800 nm wavelength, 6 μJ pulse energy, and 50 fs pulse duration. The required wavelengths in the ultra violet (UV) range were obtained by frequency doubling the output of a noncollinear optical parametric amplifier [32], which was used to convert the fundamental single wavelength freely tunable to any wavelength in the range 480–680 nm. Thus, femtosecond pulses in a wavelength range 240 nm $\leqslant \lambda \leqslant$ 340 nm were accessible. A pair of prisms was used for compensation of group velocity dispersion to achieve pulses with a temporal width of $\Delta t < 40$ fs, thus providing a high photon density at a high repetition rate. The photon flux per pulse and area was typically in the order of 10^{12} cm^{-2}. Since the focus of this paper is on the electronic structure, we only show measurements that were recorded with a single pulsed laser beam. This is not to be confused with time-resolved 2PPE, where two laser beams are employed to measure the electron dynamics.

The photoemitted electrons were collected using a time-of-flight spectrometer. A positive bias voltage <1 V was used to extract and to detect electrons with low kinetic energies that would otherwise not reach the detector. A second commercial LayTec EpiRAS RA spectrometer was mounted on the same UHV chamber where the 2PPE measurements were conducted, thus allowing us to measure under identical conditions.

III. RESULTS AND DISCUSSION

A. Characterization with RAS

RA spectra of the P- and Ga-rich surface reconstructions, before and after O_2 exposure, are shown in Fig. 1. The RAS signal is defined as

$$\frac{\Delta r}{r} = 2\frac{r_x - r_y}{r_x + r_y} \tag{1}$$

with $r_{x,y}$ being two orthogonal components of the complex reflectivity parallel to the surface plane. Here, only the real part of the complex RAS signal is analyzed. Since the crystal structure of GaP is cubic, no polarization-dependent behavior is expected for purely bulk-related transitions. Features in the RA spectra can thus be associated with electronic transitions [29] that are either directly related to surface states or involve surface-modified bulk states [33].

The RA spectra of the samples investigated here show excellent qualitative agreement with previous MOVPE-grown samples [25,28,34,35], insuring well-defined and reproducible surfaces available to the 2PPE experiments. The Ga-rich surface is extremely sensitive to background pressure even in UHV, so that surface state-related features start to decrease continually after preparation. The RAS signal of the Ga-rich surface, shown in Fig. 1, was measured after the 2PPE experiments. This results in surface state-related peaks with an unavoidable lower amplitude, compared to measurements shown in former publications that were performed directly after preparation [31]. To ensure that no spectral shifts occurred, RA spectra were also recorded in between 2PPE measurements.

DFT-LDA calculations by Schmidt *et al.* [12] and Hahn *et al.* [13] revealed that the features up to $h\nu \approx 3.7$ eV are completely related to surface-state transitions. We see clearly that these features vanish after O_2 exposure for both surface reconstructions, which indicates the entire quenching

of surface states. For energies $h\nu \geqslant 3.7$ eV we also noticed a drop in amplitude and a change in shape, but no complete disappearance of the signal. This also agrees with the calculations [12,13] that predicted a signal in this energy region, which is related to surface-modified bulk transitions located at atomic layers below the surface [30] and thus likely unaffected by oxygen exposure. For the Ga-rich surface, the peak at approximately 4.7 eV, in particular, was assigned to an anisotropic modification of the E_0' bulk transition [12]. The change of the broad feature between 3.5 and 4.5 eV at the Ga-rich surface and its slight shift towards higher energies could be due to the formation of Ga-O-Ga or Ga-O-P bonds [17,19], but is not discussed here.

B. Band alignment

To allocate surface states, appearing in the 2PPE spectra energetically with respect to the bulk bands, it is necessary to know the position of the Fermi level relative to the bulk bands at the surface. In our case, this was not trivial, since we did deliberately not dope the samples to ensure a surface quality as high as possible. With capacitance-voltage (CV) measurements we found $n < 10^{15}$ cm^{-3} for the background doping level that is determined by impurities, introduced during growth or diffusing from the sulfur doped substrate. However, at such low doping concentrations the uncertainty of the CV method is too high for our purpose.

We therefore grew a reference sample with a well-defined p doping of $p = 5 \times 10^{17}$ cm^{-3}, using diethylzinc (DEZn) as doping precursor. In this case, the position of the Fermi level E_F is well defined and was calculated to be 0.2 eV above the valence-band maximum (VBM) by solving

$$p = \int_{-\infty}^{\infty} \mathrm{DOS}(E) f(E, E_F) dE \qquad (2)$$

numerically for E_F. Here, $f(E, E_F)$ is the Fermi distribution at $T = 300$ K and DOS(E) the density of states of the band edges, derived using the effective-mass approximation with literature parameters [36].

Due to the different doping levels, the 2PPE kinetic-energy spectra of the differently doped samples appear shifted with respect to each other. This allowed us to allocate the position of the Fermi level in a 2PPE spectrum of the undoped samples, simply by shifting it in energy until it matches the spectrum of the p-type sample. With a measured shift of $\Delta E = 1.61$ eV and a band-gap spacing [37] of 2.26 eV, we find that the Fermi level of the undoped sample is located approximately 0.45 eV below the level of the conduction-band minimum E_{CBM}. In turn, based on calculations of the density of states and using an approximation of the conduction-band minimum (CBM) [36], Eq. (2) (with n for p) returned a background doping concentration of $n \approx 10^{14}$ cm^{-3}, in agreement with the CV-profiling measurements.

We noted that the spectrum of the undoped sample shifts to lower kinetic energies with higher laser intensities, following a logarithmic dependence that is typical for photovoltage. This is most pronounced when measuring with laser intensities <20 μW. We explain this by an upward surface band bending at the undoped samples, which is compensated for by increasing light intensities through surface photovoltage [26,38–40] (SPV). For the p-type sample, we assume flat-band conditions, as no such shift could be observed here.

The comparison between spectra of p-type and undoped samples could not be performed for each single measurement. In order to have comparable conditions, we kept the laser intensity considerably high for all measurements. A nonuniform compensation of the band bending due to changes in SPV for different measurements would introduce an error in the energy scaling. We estimate the resulting tolerance in determining the Fermi-level position to $\Delta(E_{\mathrm{CBM}} - E_F) \approx 0.15$ eV, limited by the uncertainty of the doping concentration at the p-type sample and possible variations of the SPV. This results in an overall accuracy of $\Delta E \approx 0.21$ eV for allocating a 2PPE signal energetically with respect to the bulk bands. Here also the broadening due to the spectral width of the laser pulse and the resolution for the kinetic energy contribute.

C. Detection of surface states

In the 2PPE measurements presented here, the absorption of two photons is necessary to lift an electron from occupied states (initial states) to states above the vacuum level (final states) since the energy of each photon is well below the ionization energy. This occurs either as a coherent two-photon process, or in two steps by first populating empty states (intermediate states) with one photon and then promoting those electrons to states above the vacuum level via a second photon. For the absorption of two photons by one electron, a sufficiently high photon density is required. This is provided here by using ultrashort laser pulses (duration <40 fs), whereby the absorption of both photons happens during the length of one laser pulse.

Discrimination between bulk- and surface-related features was achieved by measuring kinetic-energy spectra of both the Ga-rich and the P-rich GaP(100) surface reconstructions before and after O_2 exposure. Dangling-bond surface states are quenched completely when the surface is exposed to O_2, as has been reported for other semiconductors [41–43], and as is also indicated by the RAS measurements (cf. Fig. 1). 2PPE spectra, recorded with a photon energy of $h\nu = 4.59$ eV, are compared in Fig. 2(a). The prominent peak at $E_{\mathrm{kin}} \approx 2.2$ eV, that is clearly visible in all measurements and remains unaffected after O_2 exposure, was used as a reference for normalization. Here and in the following, the kinetic-energy scale denotes the energy of the electrons directly after photoemission and refers to the low-energy cutoff of the spectrum.

Apart from the secondary electron edge, giving the highest count rate at the low-energy side of the spectra, up to four prominent features can be distinguished. One peak at $E_{\mathrm{kin}} \approx 1$ eV, labeled $\boldsymbol{A}$, could only be observed at the Ga-rich surface unexposed to O_2 and is consequently attributed to a surface state of this particular surface. Two peaks, labeled $\boldsymbol{B}$ and $\boldsymbol{C}$, at $E_{\mathrm{kin}} \approx 2.2$ eV and $E_{\mathrm{kin}} \approx 3$ eV, respectively, remained clearly visible prior to and after O_2 surface treatment and are therefore assigned to bulk transitions. At the high-energy edge, before O_2 exposure, the Ga-rich surface shows a peak at $E_{\mathrm{kin}} \approx 3.6$ eV, referred to as $\boldsymbol{D_{Ga}}$, whereas the P-rich surface shows a shoulder at $E_{\mathrm{kin}} \approx 3.3$ eV, labeled $\boldsymbol{D_P}$. Since both surface reconstructions show a significantly different behavior in this energy region, $\boldsymbol{D_P}$ and $\boldsymbol{D_{Ga}}$ can be clearly assigned to surface-related states of each particular surface reconstruction.

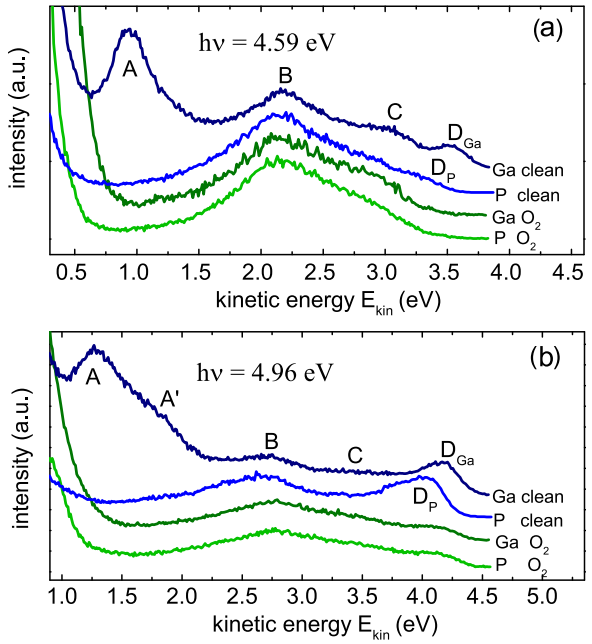

FIG. 2. (Color online) Spectra of both surface reconstructions, indicated here with Ga and P, respectively, before and after oxygen exposure. The excitation energies were (a) $h\nu = 4.59$ eV and (b) $h\nu = 4.96$ eV. The spectra are normalized to the peak ***B*** and shifted with respect to the y axis for better visibility.

D. Energetic allocation of surface states

In the following, we intend to allocate the observed surface states energetically within the band diagram of GaP that is shown in a simplified form in the middle of Fig. 3 for $\vec{k}$ values between Γ and X, where $\vec{k}$ is orthogonal to the surface. In this figure we also summarize the surface-state positions and the evolution of the corresponding peaks in the 2PPE kinetic-energy spectra. For detailed information on the band structure of GaP see, e.g., Refs. [37,45,46].

We can calculate the intermediate-state energy E_i from the applied photon energy and measured kinetic energy. In Fig. 3 this is schematically shown as the position where the arrowhead depicting the first photon meets the origin of the second arrow that figuratively lifts the second photon above the vacuum level. Here, as reference energy we preferably use E_{CBM} instead of the vacuum level E_{Vac}, which is used as reference for the kinetic energy. This is done by using

$$E_i - E_{\mathrm{CBM}} = \phi + E_{\mathrm{kin}} - h\nu - (E_{\mathrm{CBM}} - E_F), \qquad (3)$$

with ϕ being the work function of the sample, measured via the low-energy cutoff.

In Fig. 4, spectra for different photon energies at the Ga-rich surface are shown. Energy scaling has been accomplished according to Eq. (3). A shoulder next to ***A*** appears for excitation energies $h\nu \geqslant 4.77$ eV and is labeled ***A′***. Comparing spectra of both surface reconstructions before and after oxygen exposure in Fig. 2(b) for $h\nu = 4.96$ eV reveals that ***A′*** also appears only at the clean Ga-rich surface, indicating a relation to surface states.

Figure 5 displays the intermediate-state energy of all peaks for both surfaces, plotted versus the excitation energy. The positions of the peaks were determined using a fit with multiple Gaussians and a monoexponential background for the secondary electron edge, as shown exemplarily in the inset of Fig. 4. Error bars, representing the uncertainty in fitting the spectra, would be smaller than the size of the symbols.

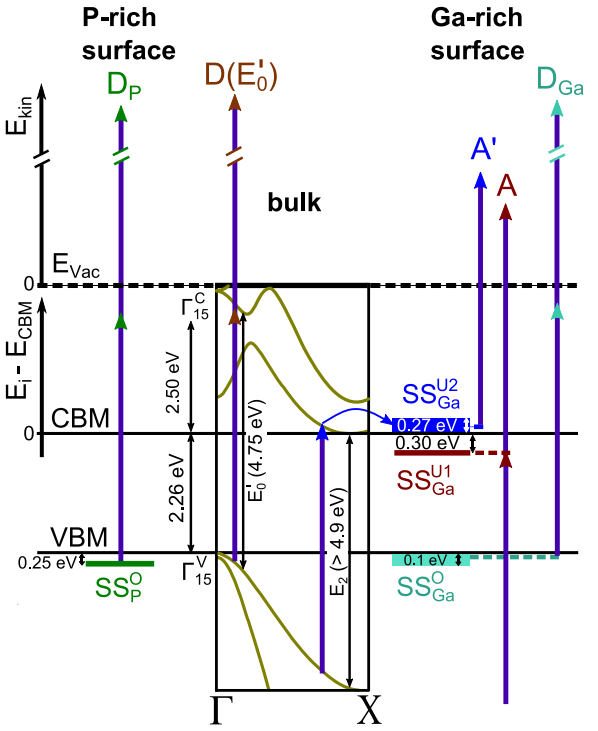

FIG. 3. (Color online) Schematics of the surface-state energies relative to the bulk band edges on the left-hand side for the P-rich surface and on the right-hand side for the Ga-rich surface. Vertical arrows correspond to photons of $h\nu \approx 4.86$ eV and indicate transitions that lead to peaks in the spectra. The bulk band structure in the middle, sketched according to Ref. [44], illustrates the bulk transitions, discussed in the text. The curved arrow indicates a scattering process. Peaks ***B*** and ***C*** have been left out, since their origin could not be allocated unambiguously.

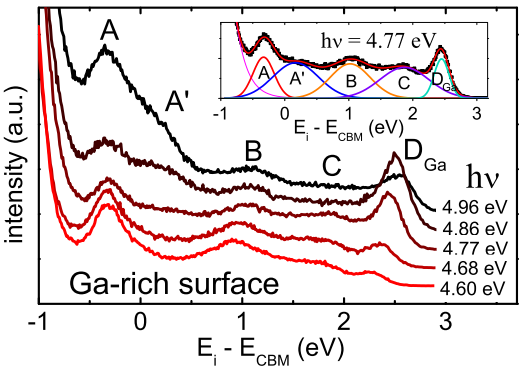

FIG. 4. (Color online) 2PPE spectra of the clean Ga-rich surface for different excitation energies. The energy scale represents the intermediate-state energy with respect to the CBM. The inset shows the multiple gauss fit with a monoexponential background, which was used to determine the positions of the peaks, exemplarily for the spectrum recorded with $h\nu = 4.77$ eV.

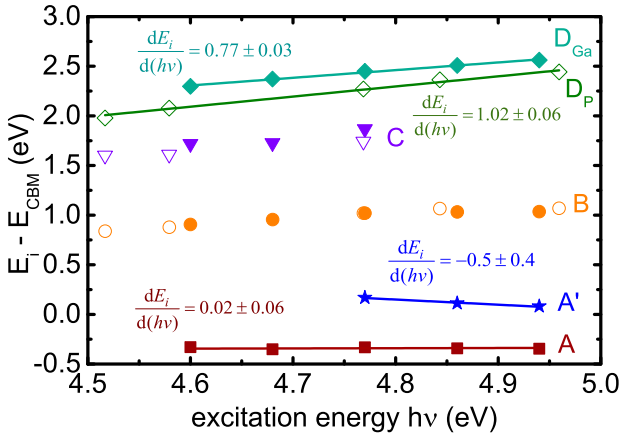

FIG. 5. (Color online) Intermediate-state energy with respect to the CBM for different peaks of the Ga-rich (filled symbols) and P-rich (open symbols) surface in dependence of the excitation energies. The energy scale is calculated according to Eq. (3). Values for $\boldsymbol{A'}$ and $\boldsymbol{C}$ are only plotted for excitation energies, where unambiguous extraction of the peak position was possible.

The uncertainty due to the band alignment as discussed in Sec. III B is not included, as it would lead to an identical shift of all values.

Surface-state bands are two dimensional and do not show any dispersion orthogonal to the surface. The dispersion parallel to the surface can be disregarded here as only electrons are detected that are photoemitted normal to the surface. Thus, unoccupied surface states can be clearly identified as peaks which stay at the same intermediate state energy when the photon energy is varied [47] (see again Fig. 3). For an occupied surface state, on the other hand, a peak in the 2PPE spectrum arises due to coherent two-photon absorption. The energy of the corresponding virtual intermediate state then depends linear on the excitation energy [47] with a slope of $\frac{dE_i}{d(h\nu)} = 1$.

The slope values of the surface-state-related peaks were extracted using linear regression and are shown in Fig. 5, next to the fitting curves. We found $\frac{dE_i}{d(h\nu)} \approx 0$ for $\boldsymbol{A}$, indicating that this peak corresponds to an unoccupied surface state that is transiently populated within the laser pulse duration in the 2PPE experiment. This state is energetically allocated in the bulk band gap, approximately 0.3 eV below the CBM and will be referred to as SS^{U1}_{Ga} in the following.

To facilitate the comprehension of the following analysis, we refer the reader to Fig. 3 where the results have been illustrated graphically. Our finding of $\frac{dE_i}{d(h\nu)} < 0$ for $\boldsymbol{A'}$ cannot be explained by pure surface-state transitions, which means that bulk states with dispersion normal to the surface are involved. The only unoccupied bulk states in the corresponding intermediate-state energy range (80–270 meV above the CBM) are in the vicinity of the high-symmetrical X point of the Brillouin zone. Reported values [45] for the direct transition E_2 from X^v_5 to X^c_1 in this energy region are in the range of 4.9–5.3 eV. This is clearly energetically above the here-observed threshold energy of $h\nu \approx 4.77$ eV for the appearance of $\boldsymbol{A'}$. However, transitions along the $\Gamma \rightarrow X$ direction close to the X valley are possible at lower photon energies since the distance between valence and conduction band narrows when moving from X towards Γ (cf. Fig. 3). When using higher photon energies, the bulk transition shifts closer to X in reciprocal space and energetically lower states are populated, which explains the measured $\frac{dE_i}{d(h\nu)} < 0$ for $\boldsymbol{A'}$.

As $\boldsymbol{A'}$ could not be observed after O_2 exposure or at the P-rich surface, we assume that electrons in bulk states close to the CBM are not directly visible in the 2PPE spectra. This can be explained by the absence of final states which are allowed in terms of dipole selection rules. Photoemission from surface states on the other hand can be strongly enhanced due to different selection rules. We attribute the appearance of $\boldsymbol{A'}$ at the clean Ga-rich surface to extremely fast scattering into isoenergetic surface states with a high photoemission probability. These states are called SS^{U2}_{Ga} in the following (cf. Fig. 3).

For the surface-state-related peak $\boldsymbol{D_P}$, we find $\frac{dE_i}{d(h\nu)} = 1.02 \pm 0.06$. We thus relate $\boldsymbol{D_P}$ to an occupied surface state at the P-rich surface that lies approximately 0.25 eV below the VBM and will be labeled SS^{O}_{P}. The energetic position of the initial state is derived by subtracting $h\nu$ from the intermediate-state energy as deduced from Eq. (3). For the Ga-rich surface, the dispersion of $\boldsymbol{D_{Ga}}$ exhibits $\frac{dE_i}{d(h\nu)} = 0.77 \pm 0.03$ eV, which is untypical for peaks related to nondispersing states and thus indicates the involvement of bulk states. The corresponding occupied surface states are to be allocated 0.0–0.1 eV below the VBM and will be labeled SS^{O}_{Ga}.

We noticed a shoulder at $E_{\mathrm{kin}} = 4.2$ eV in the spectra of the O_2-exposed samples, recorded with a photon energy of $h\nu = 4.96$ eV (cf. Fig. 2). Since this shoulder occurs at both surface reconstructions and is independent of oxygen exposure, we attribute it to a bulk transition. Variation of the excitation energy at the O_2-exposed mixed-dimer surface reveals that this shoulder appears only for $h\nu \geqslant 4.76$ eV (cf. Fig. 2). This threshold energy for the proposed corresponding bulk transition is in very good agreement with the transition energy $E'_0 \approx 4.75$ eV [37] between the VBM (Γ^v_{15}) and Γ^c_{15}. The states at Γ^c_{15} are expected [37] to lie about 2.5 eV above the CBM (see also Fig. 3), which also agrees with the 2.4–2.6 eV measured here. The bulk intermediate states, which contribute to $\boldsymbol{B}$ and $\boldsymbol{C}$, are located in a range 0.84–1.07 eV and 1.60–1.87 eV respectively above the CBM. An unambiguous assignment to certain points of the Brillouin zone was not possible, as a large variety of transitions is possible at the photon energies that have been employed.

We compare the results to theoretical calculations found in literature. It is important to keep in mind that the surface states we probed with 2PPE (cf. Fig. 3) are solely located in the center of the surface Brillouin zone ($\bar{\Gamma}$), as only electrons are detected that are photoemitted normal to the surface. Schmidt *et al.* [12] and Hahn *et al.* [13] performed DFT-LDA calculations for the Ga-rich and P-rich surface reconstructions that are investigated here, and used their results to simulate RA spectra. Diagrams of the calculated surface electronic structures can be found in Refs. [12,13]. An underestimation of the calculated band gaps was treated by employing the GW approximation for the Ga-rich surface [12], while for the P-rich surface reconstruction Hahn *et al.* indicate that the self-energy was

approximated by a rigid shift in energy [13]. Since perfect agreement of the experimental and calculated RA spectra could not be achieved, the accuracy of the corresponding calculated surface-state energies might be limited. However, since the main features of the experimental RA spectra could be simply reproduced, we expect the calculated values to suffice for a qualitative comparison.

Our finding of an occupied surface state SS^{O}_{Ga}, 0.0–0.1 eV below the VBM, at the Ga-rich surface, agrees well with an occupied surface state $V1$ (related to the phosphorus dangling bond) that was calculated to be located slightly above the VBM [12]. The unoccupied surface state SS^{U1}_{Ga}, 0.3 eV below the CBM, is in accordance with a predicted series of unoccupied states C1–C5 in the upper part of the bulk band gap [12] (related to dangling bonds of second layer cations). The appearance of the peak $\boldsymbol{A'}$, which is specific for the Ga-rich surface and associated with SS^{U2}_{Ga} slightly above the CBM, might also be related to C1–C5.

Disappearance of the unoccupied surface-state peaks after O_2 exposure also agrees well with calculations of Wood *et al.* for the Ga-rich surface, where a strong quenching of near CBM surface states was predicted [17] for chemisorption of O_2. However, an enhancement of occupied surface states close to the VBM that was predicted by Wood *et al.* is in contradiction to the quenching of the occupied surface states observed here. For the P-rich reconstruction, the surface state SS^{O}_{P}, 0.25 eV below the CBM, can be identified as a dangling-bond state of the lower phosphorus atom that has also been calculated in the vicinity of the VBM [13].

E. Comparison with RAS

The geometric anisotropy of both GaP(100) surface reconstructions suggests that corresponding surface-state-related transitions also show a polarization dependence. The energetic differences between the observed occupied and unoccupied surface states, as well as between the occupied surface states and the CBM, have been indicated with vertical bars in Fig. 1. Transitions between these states will appear in the corresponding RA spectra, if they are allowed in terms of dipole selection rules and anisotropic. We see that the observed differences in the surface electronic structure suitably explain the different shapes of the RAS curves for the Ga- and the P-rich surface reconstructions. RAS peaks are not necessarily centered exactly at the energy of the corresponding transitions, since the RA signal arises due to a complex interplay between the surface and bulk dielectric functions [29].

We investigated the polarization dependence of surface related transitions explicitly by recording 2PPE spectra of the Ga-rich surface with laser beams of different polarization but constant intensity and $h\nu = 4.86$ eV. The results are shown in Fig. 6(a). For p-polarized light, one component of the electric-field vector is parallel to the $[0\bar{1}1]$ crystal axis and lying in the surface plane. The influence of the other field component that is perpendicular to the surface was found to be negligible by varying the angle of incidence. For s-polarized light, the whole field vector is parallel to [011] and thus also lies in the surface plane. A drop in intensity for the surface state-related peaks, as compared to the spectra in Fig. 4,

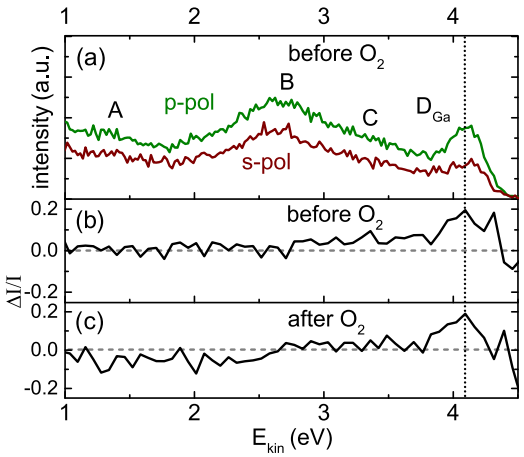

FIG. 6. (Color online) (a) 2PPE spectra of the Ga-rich surface recorded with a photon energy of $h\nu = 4.86$ eV with p and s polarized laser light of same intensity, respectively, before oxygen exposure of the sample. (b) Anisotropy of the signal based on the assumption that peak $\boldsymbol{B}$ is isotropic for the sample before oxygen exposure and (c) after oxygen exposure. The vertical dashed line marks the position of $\boldsymbol{D_{\mathrm{Ga}}}$.

is attributed to the fact that these measurements have not been conducted immediately after preparation. Thus, parts of the highly sensitive surface states might have been already quenched, as discussed in Sec. III A.

The spectrum with p-polarized light shows generally a higher photoelectron yield, which can be mostly ascribed to the higher reflection of s-polarized light under an incidence angle of 45°. However, the difference in intensity is not as pronounced as expected by applying the Fresnel equations, probably because most of the 2PPE signal stems directly from the surface where the Fresnel theory is not sufficient to describe the intensities correctly. Both spectra therefore need to be normalized to an isotropic feature. In the following, peak $\boldsymbol{B}$ is chosen as an isotropic reference, since all our measurements indicate that it is purely bulk related. Based on this assumption, we evaluate the polarization-dependent measurements by defining

$$\frac{\Delta I}{I} = \frac{I_{p-\mathrm{pol}} - I_{s-\mathrm{pol}}}{I_{p-\mathrm{pol}} + I_{s-\mathrm{pol}}} \tag{4}$$

as the anisotropy of the signal, being 1 (−1) for a signal only appearing with p-polarized (s-polarized) light and zero for an isotropic signal. In Fig. 6(b), we see that the signal is isotropic over the whole energetic range, except for a significant increase centered at around 4.1 eV, which agrees with the position of the peak $\boldsymbol{D_{\mathrm{Ga}}}$. This anisotropy of $\boldsymbol{D_{\mathrm{Ga}}}$ hints to the existence of at least one polarization-dependent transition involved in the evolution of this peak that was above assigned to both occupied surface state SS^{O}_{Ga} and the bulk transition E'_0 between Γ^{v}_{15} and Γ^{c}_{15} (cf. Fig. 3).

To distinguish whether the anisotropy stems from the bulk or the surface-state component of $\boldsymbol{D_{\mathrm{Ga}}}$ or both, we repeated the polarization-dependent 2PPE measurement after quenching

the surface-state contribution with oxygen, so that

$$\left.\frac{\Delta I}{I}\right|_{\text{clean}} = \frac{I^{\text{bulk}}_{p-\text{pol}} + I^{SS}_{p-\text{pol}} - I^{\text{bulk}}_{s-\text{pol}} - I^{SS}_{s-\text{pol}}}{I^{\text{bulk}}_{p-\text{pol}} + I^{SS}_{p-\text{pol}} + I^{\text{bulk}}_{s-\text{pol}} + I^{SS}_{s-\text{pol}}}, \quad (5)$$

$$\left.\frac{\Delta I}{I}\right|_{O_2} = \frac{I^{\text{bulk}}_{p-\text{pol}} - I^{\text{bulk}}_{s-\text{pol}}}{I^{\text{bulk}}_{p-\text{pol}} + I^{\text{bulk}}_{s-\text{pol}}}. \quad (6)$$

Here I^{bulk} and I^{SS} are the bulk and surface-state contributions to $\boldsymbol{D}_{\mathbf{Ga}}$, respectively.

It follows, that for a polarization-independent surface-state contribution ($I^{SS}_{p-\text{pol}} = I^{SS}_{s-\text{pol}}$), a significantly stronger anisotropy is expected for the O_2-exposed sample. However, such a change in anisotropy could not be observed, as seen in Fig. 6(c), while the amplitude of $\boldsymbol{D}_{\mathbf{Ga}}$ drops considerably after O_2 exposure, as discussed earlier. Thus, the surface-state contribution to $\boldsymbol{D}_{\mathbf{Ga}}$, involving SS^{O}_{Ga}, is anisotropic with a higher transition probability for light that is polarized parallel to the Ga-P top dimers. Our finding of $\frac{dE_i}{d(h\nu)} < 1$ for this peak (cf. Fig. 5) suggests the existence of a possible direct transition between SS^{O}_{Ga} and the bulk states Γ^{c}_{15} leading to a signal that overlaps in the 2PPE spectra with the E'_0 bulk contribution.

A transition between SS^{O}_{Ga} and the bulk states Γ^{c}_{15} would be energetically close to the E'_0 transition, where Ga-rich GaP(100) exhibits a peak in the RAS signal (cf. Fig. 1). This peak also shows a significant drop in intensity after O_2 exposure, in agreement with the observed quenching of the SS^{O}_{Ga} surface states in the 2PPE measurements. The remaining amplitude of the RAS peak after O_2 exposure was previously found to result from a surface-induced optical anisotropy of the E'_0 bulk transition, by comparing experimental RAS data with DFT based simulations [30]. This is in line with the observed anisotropy of the bulk contribution to the peak $\boldsymbol{D}_{\mathbf{Ga}}$ in the 2PPE spectra, which we also associate with the transition E'_0, as discussed above.

For the bulk as well as for the surface-state related component of $\boldsymbol{D}_{\mathbf{Ga}}$, light polarized parallel to the $[0\bar{1}1]$-crystal axis leads to a stronger signal. Our results show that RAS and 2PPE work well as complementary methods. While the former method is easy to employ and sensitive to surface state-related transitions, the latter method can directly address these transitions and allocate the corresponding states energetically with respect to the bulk band edges.

IV. CONCLUSION

2PPE spectroscopy and RAS have been utilized to investigate the electronic structures of the Ga-rich (2×4) and the hydrogen-terminated P-rich $(2 \times 2)/c(4 \times 2)$ reconstruction of the GaP(100) surface. For both surfaces, occupied surface states were detected in the vicinity of the VBM. Their energies complement theoretical calculations that describe dangling bonds at the phosphorus atoms. The Ga-rich surface reconstruction exhibited unoccupied states in the vicinity of the CBM, which presumably originate from the cation atoms of the second layer of the surface. All of these surface states are quenched when the respective surface is exposed to oxygen.

The photon energy used in the 2PPE experiments was tuned to match the E'_0 bulk transition energy between the Γ^{v}_{15} and Γ^{c}_{15} states. Polarization-dependent measurements revealed an anisotropic behavior of this transition in agreement with observations from RA spectra and also with theoretical calculations. We found a correlation between features in the RA spectra, and the energy spacings between surface-related states and between surface- and bulk-related states, which were detected with 2PPE. Future 2PPE studies might be conducted with a second beam of a different photon energy. Thus, optical surface-state transitions that were indicated in RA spectra can be selectively photoexcited to allocate the energetic positions of the corresponding surface states.

ACKNOWLEDGMENTS

This work was supported by the BMBF (Project No. 03SF0404A). P.S. would like to thank K. Schwarzburg for valuable discussions.

[1] M. G. Walter, E. L. Warren, J. R. McKone, S. W. Böttcher, Q. Mi, E. A. Santori, and N. S. Lewis, Chem. Rev. **110**, 6446 (2010).
[2] K. S. Joya, Y. F. Joya, K. Ocakoglu, and R. van de Krol, Angew. Chem. Int. Ed. **52**, 10426 (2013).
[3] B. Kaiser, D. Fertig, J. Ziegler, J. Klett, S. Hoch, and W. Jaegermann, Chem. Phys. Chem. **13**, 3053 (2012).
[4] H. Döscher, T. Hannappel, B. Kunert, A. Beyer, K. Volz, and W. Stolz, Appl. Phys. Lett. **93**, 172110 (2008).
[5] J. Wolters, A. W. Schell, G. Kewes, N. Nüsse, M. Schoengen, H. Döscher, T. Hannappel, B. Löchel, M. Barth, and O. Benson, Appl. Phys. Lett. **97**, 141108 (2010).
[6] S. Hu, C. Xiang, S. Haussener, A. D. Berger, and N. S. Lewis, Energy Environ. Sci. **6**, 2984 (2013).
[7] J. F. Geisz, J. Olson, D. Friedman, K. Jones, R. Reedy, and M. Romero, in *Conference Record of the Thirty-first IEEE Photovoltaic Specialists Conference*, 2005 (IEEE, New York, 2005), pp. 695–698.
[8] H. Döscher, O. Supplie, M. M. May, P. Sippel, C. Heine, A. G. Muoz, R. Eichberger, H.-J. Lewerenz, and T. Hannappel, Chem. Phys. Chem. **13**, 2899 (2012).
[9] A. M. Frisch, W. G. Schmidt, J. Bernholc, M. Pristovsek, N. Esser, and W. Richter, Phys. Rev. B **60**, 2488 (1999).
[10] N. Esser, W. G. Schmidt, J. Bernholc, A. M. Frisch, P. Vogt, M. Zorn, M. Pristovsek, W. Richter, F. Bechstedt, T. Hannappel, and S. Visbeck, J. Vac. Sci. Technol. **17**, 1691 (1999).
[11] L. Töben, T. Hannappel, K. Möller, H. J. Crawack, C. Pettenkofer, and F. Willig, Surf. Sci. **494**, L755 (2001).
[12] W. G. Schmidt, J. Bernholc, and F. Bechstedt, Appl. Surf. Sci. **166**, 179 (2000).
[13] P. H. Hahn, W. G. Schmidt, F. Bechstedt, O. Pulci, and R. Del Sole, Phys. Rev. B **68**, 033311 (2003).

[14] D. Li, K. Liu, H. Xiao, H. Dong, and X. Zu, J. Alloy. Compd. **440**, 229 (2007).
[15] Y. Fukuda, M. Shimomura, N. Sanada, and M. Nagoshi, J. Appl. Phys. **76**, 3632 (1994).
[16] N. Kadotani, M. Shimomura, and Y. Fukuda, Phys. Rev. B **70**, 165323 (2004).
[17] B. C. Wood, T. Ogitsu, and E. Schwegler, J. Chem. Phys. **136**, 064705 (2012).
[18] S. Jeon, H. Kim, W. A. Goddard, and H. A. Atwater, J. Phys. Chem. C **116**, 17604 (2012).
[19] M. M. May, O. Supplie, C. Höhn, R. v. d. Krol, H.-J. Lewerenz, and T. Hannappel, New J. Phys. **15**, 103003 (2013).
[20] H. Döscher, K. Möller, and T. Hannappel, J. Cryst. Growth **318**, 372 (2011).
[21] H. Döscher and T. Hannappel, J. Appl. Phys. **107**, 123523 (2010).
[22] M. Weinelt, M. Kutschera, T. Fauster, and M. Rohlfing, Phys. Rev. Lett. **92**, 126801 (2004).
[23] T. Ichibayashi and K. Tanimura, Phys. Rev. Lett. **102**, 087403 (2009).
[24] C. Eickhoff, M. Teichmann, and M. Weinelt, Phys. Rev. Lett. **107**, 176804 (2011).
[25] A. Okano, R. K. R. Thoma, G. P. Williams, and R. T. Williams, Phys. Rev. B **52**, 14789 (1995).
[26] C. A. Schmuttenmaer, C. Cameron Miller, J. W. Herman, J. Cao, D. A. Mantell, Y. Gao, and R. J. D. Miller, Chem. Phys. **205**, 91 (1996).
[27] L. Töben, T. Hannappel, R. Eichberger, K. Möller, L. Gundlach, R. Ernstorfer, and F. Willig, J. Cryst. Growth **248**, 206 (2003).
[28] T. Hannappel, S. Visbeck, L. Töben, and F. Willig, Rev. Sci. Instrum. **75**, 1297 (2004).
[29] P. Weightman, D. S. Martin, R. J. Cole, and T. Farrell, Rep. Prog. Phys. **68**, 1251 (2005).
[30] W. G. Schmidt, N. Esser, A. M. Frisch, P. Vogt, J. Bernholc, F. Bechstedt, M. Zorn, T. Hannappel, S. Visbeck, F. Willig, and W. Richter, Phys. Rev. B **61**, R16335 (2000).
[31] T. Hannappel, L. Töben, K. Möller, and F. Willig, J. Electron. Mater. **30**, 1425 (2001).
[32] L. Gundlach, R. Ernstorfer, E. Riedle, R. Eichberger, and F. Willig, Appl. Phys. B **80**, 727 (2005).
[33] S. Visbeck, T. Hannappel, M. Zorn, J.-T. Zettler, and F. Willig, Phys. Rev. B **63**, 245303 (2001).
[34] X. Lu, S. Huang, M. Diaz, R. Opila, and A. Barnett, in *2010 35th IEEE Photovoltaic Specialists Conference (PVSC)* (IEEE, New York, 2010), pp. 002079–002083.
[35] T. G. Deutsch, C. A. Koval, and J. A. Turner, J. Phys. Chem. B **110**, 25297 (2006).
[36] O. Madelung, W. von der Osten, and U. Rössler, in *Intrinsic Properties of Group (IV) Elements and (III-V), (II-VI) and I-(VII) Compounds*, edited by O. Madelung (Springer, Berlin, 1986), pp. 72–75.
[37] A. E. Yunovich, Fortschr. Phys. **23**, 317 (1975).
[38] S. J. Diol, C. C. Miller, C. A. Schmuttenmaer, J. Cao, Y. Gao, D. A. Mantell, and R. J. D. Miller, J. Phys. D **30**, 1427 (1997).
[39] M. H. Hecht, Phys. Rev. B **43**, 12102 (1991).
[40] M. Alonso, R. Cimino, and K. Horn, Phys. Rev. Lett. **64**, 1947 (1990).
[41] G. Hollinger and F. Himpsel, J. Vac. Sci. Technol. **1**, 640 (1983).
[42] R. Ludeke and A. Koma, J. Vac. Sci. Technol. **13**, 241 (1976).
[43] G. Chen, S. B. Visbeck, D. C. Law, and R. F. Hicks, J. Appl. Phys. **91**, 9362 (2002).
[44] N. Fraj, I. Sadi, S. B. Radhia, and K. Boujdaria, J. Appl. Phys. **102**, 053703 (2007).
[45] I. Vurgaftman, J. R. Meyer, and L. R. Ram-Mohan, J. Appl. Phys. **89**, 5815 (2001).
[46] J. R. Chelikowsky and M. L. Cohen, Phys. Rev. B **14**, 556 (1976).
[47] C. Kentsch, M. Kutschera, M. Weinelt, T. Fauster, and M. Rohlfing, Phys. Rev. B **65**, 035323 (2001).